Mediterranean Archaeology and Archaeometry, Vol. 15, No 3, pp. 113-121

DOI: 10.5281/zenodo.18362

THE PAINT LAYERS OF MURAL PAINTINGS AT ABYDOS TEMPLES - EGYPT: A CLOSER LOOK AT THE MATERIALS USED

Ehab Al-Emam[1*], Mohamed El-Gohary[1], Mohamed Abd El Hady[2]

[1] *Conservation dept., Sohag Univ., 82524, Sohag, Egypt*

[2] *Conservation dept., Cairo Univ., 12613, Cairo, Egypt*

Received: 01/06/2014
Accepted: 19/05/2015
Corresponding author: ehab_alemam@yahoo.com

ABSTRACT

The present study forms part of the research undertaken on the mural paintings from Abydos area in Egypt, and it is concerned with the identification of the materials used in the paint layers of these murals. The methods used in this purpose are optical microscopes (OM), scanning electron microscope with an energy dispersive X-ray unit (SEM/EDS), X-ray diffraction (XED), and Fourier transform infrared spectroscopy (FTIR). Theses methods led to that the blue color was Egyptian blue, while the green one was Egyptian green; in addition, the red and yellow colors were composed of red and yellow ochres. Finally, the binder used was gum Arabic.

KEYWORDS: Abydos, Mural paintings, Egyptian blue, Egyptian green, Red ochre, Yellow ochre, Gum Arabic, FTIR, SEM

1. INTRODUCTION

Mural paintings occupied a great status in the ancient Egyptian art; and thus they have been the main concern of the studies of the ancient Egyptian art and history. This comes from the fact that ancient Egyptian artists relied on them in depicting their daily life, in addition to honoring their deceased and gods. On the other hand, the techniques and the materials used in these mural paintings are fundamental from the point of view of conservation science, since the ancient Egyptian artists used different techniques such as reliefs (sunk-raised) and paintings over a preparatory layer (Mora et al., 1984; Robins, 2005). Furthermore, they used different colors derived from variable materials found in their surrounding nature, mostly minerals; however, they managed to manufacture pigments and used them widely; like Egyptian blue and Egyptian green pigments (Lucas & Harris, 1962; Lee, & Quirke, 2000; Hatton et al., 2008).

In this respect, this work provides detailed information about the materials used in the paint layers of mural paintings at the temples of Seti I and Ramesses II which belong to the Nineteenth Dynasty in ancient Egypt (Fig. 1).

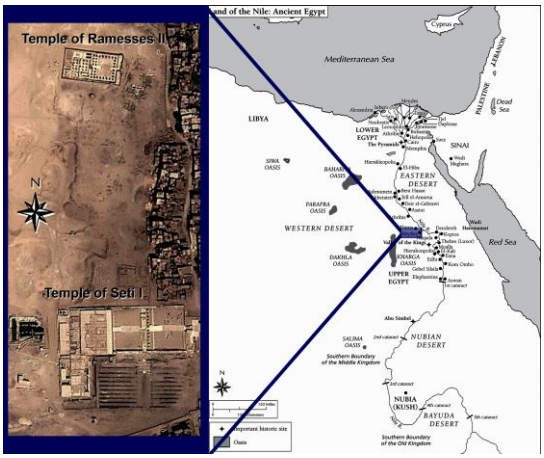

Figure 1: An Overview of the two temples.

It comes after a study on the techniques of these murals (Al-Emam et al., 2014) and will be followed by another one deals with the aspects of deterioration affecting them (Al-Emam et al., in press). Consequently, it will be easy to get the whole picture not only about these murals and their current situation but also about the mural paintings of the New Kingdom generally. These kinds of studies represent a cornerstone in the documentation of artwork in its broad scope (Dasser, 1991) which in result contribute in leading conservation plan to the right way (Mora et al., 1984; Abd El Aal, 2011). Moreover, this work will be an addition to the literatures investigating pigments and binders used in ancient Egypt with the aid of different analytical techniques (Lucas & Harris, 1962; Rickerby, 1993; Newman, & Serpico 2000; Uda et al., 2000; Wiedemann et al., 2002; Scott et al., 2009; Abd El Aal, 2011; Marey Mahmoud, 2012).

2. METHODS

Fourteen tiny samples were carefully collected from both temples in order to represent all the colors used. These samples were subjected to different techniques of examination and analyses. In order to examine the surface structure of the paint layers a stereomicroscope (BAUSH & LOMB) attached to illuminant device Jenalux 20 was equipped for this purpose, while a polarized light microscope (MEIJI Techno ML 9000) was effective in identifying the color, shape, size, and surface of the particles of pigments. The data collected from the former microscopes was by the aid of a Canon Power Shot A650 IS camera. Scanning electron microscope with an energy dispersive X-ray unit (Jeol JSM 530 attached to EDS device Oxford) offered higher magnifications of the paint layer surfaces; in addition, EDS unit provided an elemental analysis of them. An additional technique, which helped in the identification of mineralogical structure, was X-ray diffraction (Phillips PW 1840). Since the adopted technique of the mural paintings of the two temples was the tempera technique (Al-Emam et al., 2014), Fourier transform infrared spectroscopy (FTIR-8101 SHIMADZU) was used in the identification of the binder.

3. RESULTS

3.1 Blue pigment

Under stereomicroscope the samples reveal broad variety in color ranging from faded blue to darkened blue, in addition to the presence of dark blue particles (Fig. 2 A, B). Under plane polarized light (PPL), translucent particles reveal colors ranging from dark to faded blue, while some particles are masked with pale brown color. The particles are angular, irregular and platy in their shape, and characterized by broad particle size distribution ranging from fine to coarse. Some particles show rough pitted surface, and others are extremely rough. Under crossed polar light (XPL), the particles are strongly birefringent (Fig. 3 A, B, C, D).

The different blue samples examined by SEM exhibit platy particles of the pigment, which are surrounded by different particles (Fig. 4 A, B). EDS analyses exhibit the following data: sample (S6B) contains Si, Ca, S, Cu, Al, K, Mg, Na, P and Ti. The elements presented in samples (SB1) and (ROB) are Ca, Si, S, Cu, Al, Cl, K, Mg, Na and P; however, they differ in their percentages (Table 1 & Fig. 5).

Table 1: Codes, colors, and locations of the paint layer samples.

Samples' code	*Color*	*The Temple*
S6B	Blue	Seti I
SB1	Blue	Seti I
ROB	Blue	Ramesses II
S6G	Green	Ramesses II
ROG	Green	Ramesses II
S6R	Red	Seti I
RR1	Red	Ramesses II
RR	Red	Ramesses II
SY	Yellow	Seti I
S6Y	Yellow	Seti I
RKY	Yellow	Ramesses II
RY	Yellow	Ramesses II
RY1	Yellow	Ramesses II
S-Barques	Yellow & Red	Seti I

In line with the former data, XRD analyses confirm its results. Sample (S6B) provides the following minerals: the majors are gypsum, cuprorivaite and calcite, the minor is brochantite, and the traces are atacamite, paratacamite, cupro-wollastonite, anhydrite, thenardite, halite and whewellite. In addition to sample (ROB), whose major minerals are anhydrite, gypsum, cuprorivaite and brochantite, the minor is calcite, and the traces are cupro-wollastonite, atacamite, paratacamite, quartz, thenardite and halite (Fig. 6 A, B).

3.2 Green pigment

By using stereomicroscope, sample (S6G) has pale green color with large dark green and blue particles, while sample (ROG) has remarkable faded green color combined with the detachment of pigment particles in some areas (Fig. 2 C, D). In PPL, the particles are translucent and their color ranges from pale green to colorless, and some particle are silica-rich. Their shape is irregular, while their size ranges from fine to coarse. In XPL, the particles show low birefringent (Fig. 3 E, F, G, H).

SEM photomicrographs of the green pigment show particles that vary in their shape and size (Fig. 4 C, D). EDS analyses reveal that both samples, (S6G) and (ROG), are composed of the same elements which are Ca, Si, S, Cu, Al, Cl, K, Mg, Na, P and Ti.

XRD results of the analyzed samples are as follows: sample (S6G) contains cupro-wollastonite as the major, brochantite, cuprorivaite, gypsum, quartz, calcite and anhydrite as the minors, while atacamite, paratacamite, thenardite and halite as the traces. Moreover, sample (ROG) shows the major mineral as cupro-wollastonite, the minors as brochantite, calcite, anhydrite, gypsum, and the traces as cuprorivaite, atacamite, paratacamite, quartz, kieserite and halite (Fig. 6 C, D).

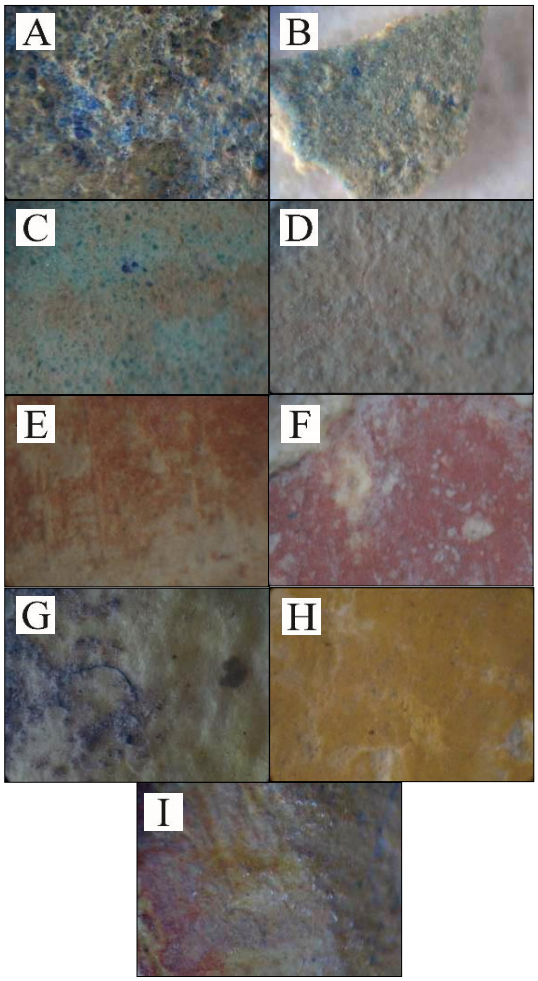

Figure 2: Optical photomacrographs of different paint layer samples under stereomicroscope 70x. *(A)* Sample (S6B) shows blue pigment with darkened areas, in addition to different particle size. *(B)* Sample (SB1) exhibits faded blue pigment with some parts tends to be green, in addition to the presence of dark blue particles. *(C)* Sample (S6G) shows green pigment with brownish areas which represent the deteriorated binder, in addition to the presence of blue particles. *(D)* Sample (ROG) exhibits strongly faded green pigment with highly detached particles. *(E)* Sample (S6R) shows degraded red pigment. *(F)* Sample (RR1) illustrates red pigment with detached area. *(G)* Sample (S6Y) exhibits yellow pigment masked with microorganisms in some areas. *(H)* Sample (RKY) shows yellow pigment suffering from detachment in some areas. *(I)* Sample (S-Barques) shows yellow/red pigment.

3.3 Red pigment

Under stereomicroscope, the samples illustrate degraded red paint layer (Fig. 2 E, F). In PPL, samples show translucent and opaque red particles clinging to particles of quartz and other impurities. The particles are characterized by irregular and angular shape; moreover, some particles are acicular. The size of particles is characterized by broad distribution ranging from very fine to very coarse. In XPL, the particles show strong birefringent (Fig. 3 I, J, K, L).

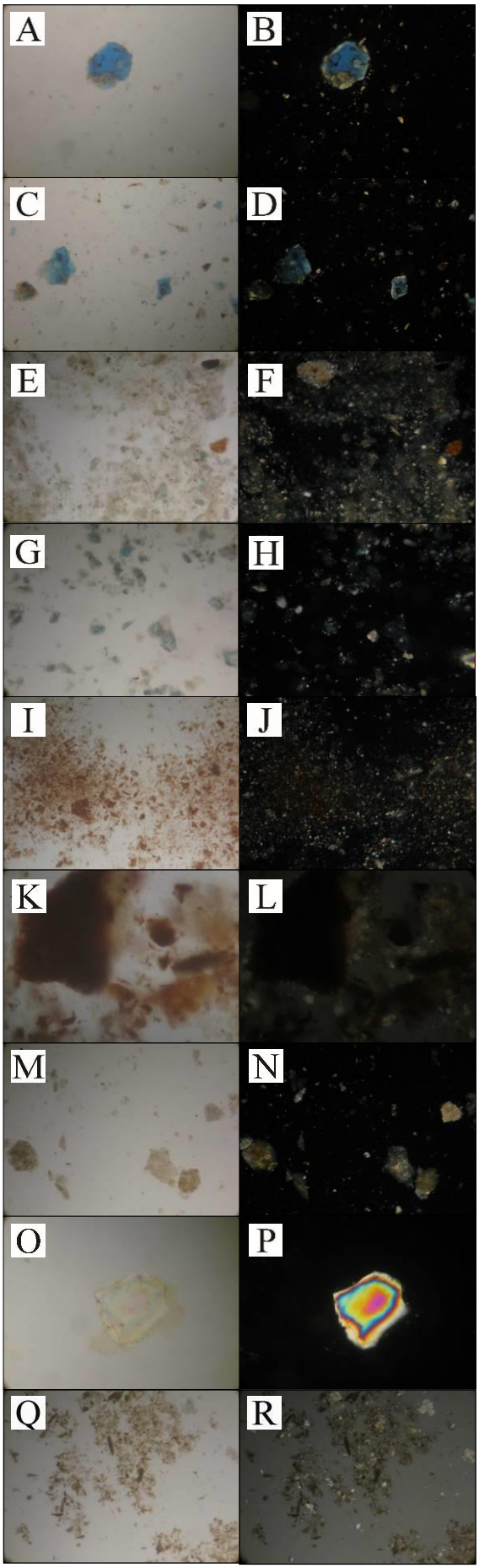

Figure 3: Optical photomicrographs of different pigment samples under polarized microscope. *(A)* Sample (SB1). PPL/100x: Irregular platy particle of Egyptian blue with a rough pitted surface. *(B)* XPL/100x: The same field under crossed polars shows high birefringent. *(C)* Sample (S6B) PPL/100x: Irregular platy particles of Egyptian blue differ greatly in their size. Some particles are masked under pale brown color; this may be from the darkened binder. *(D)* XPL/100x: The same field under crossed polars shows strong birefringent particles. *(E)* Sample (ROG) PPL/100x: Fine translucent and irregular particles of Egyptian green show faded green to colorless. The other particles may be belonging to the underneath rendering. *(F)* XPL/100x: The same field under crossed polars shows low birefringent. *(G)* Sample (S6G) PPL/100x: Translucent and irregular particles of Egyptian green show pale green color with the presence of blue particles. Some particles are silica-rich. The particles differ in their size. *(H)* XPL/100x: The same field under crossed polars shows low birefringent. *(I)* Sample (S6R) PPL/100x: Translucent irregular and angular particles of hematite clinging to particles of quartz and other impurities. The particles are greatly different in their size, and some of them are acicular. *(J)* XPL/100x: The same field under crossed polars shows strong birefringent. *(K)* Sample (RR1) PPL/100x: opaque and irregular particles of hematite-coated quartz. The particles differ in their size and shape. *(L)* XPL/100x: The same field under partially crossed polars. *(M)* Sample (SY) PPL/100x: Translucent and irregular particles of goethite show yellow-brown color with rough surface. *(N)* XPL/100x: The same field under crossed polars exhibits high birefringent. *(O)* Sample (S6Y)PPL/100x: Translucent, irregular and angular particle of pale yellow goethite-coated quartz. *(P)* XPL/100x: The same field under crossed polars. *(Q)* Sample (RKY)PPL/100x: Translucent and irregular yellow-brown goethite particles with rough surface, some of them are coated with quartz. *(R)* XPL/100x: The same field under partially crossed polars.

SEM photomicrographs show paint layers, in most samples, suffering from detachment or disintegration. In addition, these paint layers are composed of particles with different sizes and shapes (Fig. 4 E, F). EDS analyses of samples (S6R) and (RR1) present the same elements which are Al, Ca, Cl, Fe, K, Mg, Na, P, S and Si. However, sample (RR1) contains Ti unlike sample (S6R). The former elements differ in their percentages in both samples.

The XRD analyses of red samples provide the following data. The minerals presented in sample (S6R) are: gypsum as the major, hematite, microcline, calcite and anhydrite as the minors, finally, pyrite, boehmite, quartz, thenardite, kieserite and halite as the traces. Sample (RR1) shows that the major is anhydrite, the minors are calcite, gypsum and hematite, and the traces are pyrite, quartz, boehmite, kieserite and halite. While sample (RR) presents the majors as anhydrite and calcite, the minors are hematite, gypsum and microcline, and the traces are py-

rite, bohemite, quartz, kieserite and halite (Fig. 6 E, F, G).

3.4 Yellow pigment

By the examination of the yellow samples under stereomicroscope, the samples exhibit different aspects. Sample (S6Y) exhibits yellow pigment masked with microorganisms, while sample (S-Barques) shows the presence of yellow/red color. The detachments areas are obviously observed in samples (RKY) and (RY1) (Fig. 2 G, H, I). Under PPL, the color of translucent particles ranges from pale yellow to yellow-brown, while their shape is irregular and angular and some samples reveal acicular particles. The particle size ranges from very fine to very coarse. Some samples are characterized by their rough surface and others are coated with quartz. Under XPL, the particles exhibit high birefringent (Fig. 3 M, N, O, P, Q, R).

Like the red pigment, the yellow pigment under SEM shows degraded paint layer suffering from disintegration and detachment. Moreover, the samples are characterized by broad particle size distribution. Sample (S6Y) suffers from the growth of microorganisms (Fig. 4 G, H, I, J). EDS analysis of sample (SY) presents the following elements, Al, Ca, Cl, Fe, K, Mg, Na, S, Si and Ti. Samples (S6Y) and (RKY) agrees with the previous results with presence of P.

The yellow samples, which were analyzed by XRD, contain variable minerals which are as follows: the majors of sample (RKY) are anhydrite and gypsum, the minors are goethite, calcite and quartz, and the traces are pyrite, boehmite, hematite, kieserite, and halite. In sample (RY) the major minerals are gypsum, anhydrite and calcite, the minor ones are goethite and quartz, and the traces are pyrite, boehmite, hematite, kieserite and thenardite (Fig. 6 H, J).

3.5 Binder

Figure (7) represents FTIR spectrum of the samples (RY1) and (S6B) which show broad bands at 3446.2 and 3417.3 cm^{-1}. These bands are assigned to the functional group O-H which is characteristic of carbohydrates. The peaks in the range 2930-2900 cm^{-1} show C-H aliphatic asymmetrical stretching vibrational band, while the peak at 2860 cm^{-1} is the symmetrical stretching vibrational band. Moreover, the bands at 1635.8-1639 cm^{-1} are medium in their intensity and reflect asymmetric and symmetric stretching of carboxyl functional group (COO-). Also the bands at 1429.4-1453.5 cm^{-1} are attributed to COO- group. The band at 1323.3 cm^{-1} may be assigned to C-H group. The bands at the ranges 1046.5 and 1030 cm^{-1} are corresponding to C-O stretching band which is characteristic for polysaccharides. The intensity of these bands is nearly equal to that of the broad band at 3400 cm^{-1}.

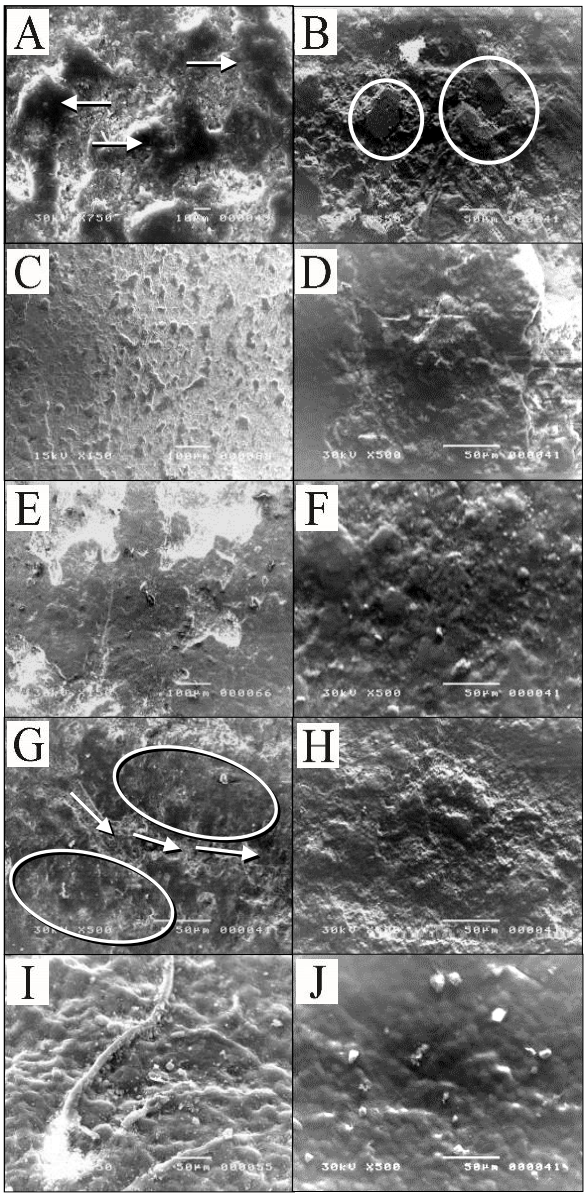

Figure 4: SEM photomicrographs of different paint layers. *(A)* Sample (S6B): the arrows point to the darkened areas of the paint layer 750x. *(B)* Sample (S6B) under back scattered electrons "BSE" shows platy particles of Egyptian blue 350x. *(C)* Sample (S6G): the dark parts represent the particles of Egyptian green 150x. *(D)* Sample (S6G) under BSE 500x. *(E)* Sample (S6R): the grey areas represent the sound parts of the paint layer, while the areas that tend to be white represent the detached parts 150x. *(F)* Sample (S6R) under BSE 500x. *(G)* Sample (RKY), the circles represent the sound areas of the paint layer, while the arrows represent the degraded areas 500x. *(H)* Sample (RKY) under BSE 500x. *(I)* Sample (S6Y) illustrates the growth of hyphae within the paint layer 350x. *(J)* Sample (S6Y) under BSE 500x.

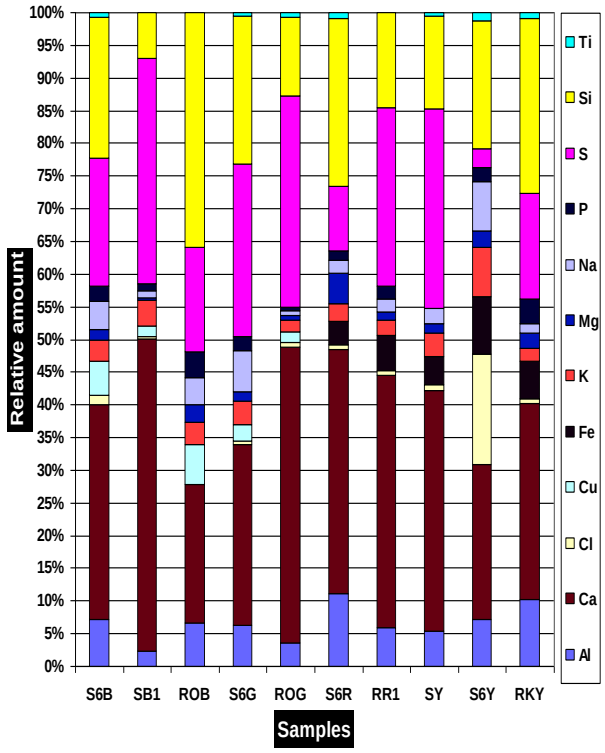

Figure 5: EDS microanalyses results of the paint layer samples.

4. DISCUSSION

4.1 Blue pigment

PLM photomicrographs reveal the remarkable platy shape of Egyptian blue (Canti & Heathcote, 2002). EDS analysis introduces the main elements of the Egyptian blue pigment Ca, Si and Cu, in addition, XRD analysis confirms these results with the existence of cuprorivaite $CaCuSi_4O_{10}$ the main compound of Egyptian blue. It should be stated that Egyptian blue is a synthetic pigments manufactured by fusing a mixture of lime (limestone powder), silica (quartz), copper source (copper alloy or malachite), and an alkali flux (soda ash) to temperatures at the range 850-1000° C (Bianchetti et al., 2000; Canti & Heathcote, 2002; Mazzocchin et al., 2004). The appearance of some particles masked with pale brown color could be assigned to the effect of the darkened binder (Al-Emam et al., in press). The samples contain variable amounts of gypsum, calcite, anhydrite and quartz. These minerals can be attributed to the rendering layer underneath the paint layer. However, Attia (1995) states that the high percentage of quartz is attributed to the addition of high amount of silica during the preparation of the pigment. In addition to the common salts thenardite and halite, one sample contains whewellite (hydrated calcium oxalate) which goes with the results presented by Pavlidou et al. (2008) who found calcium oxalate in an Egyptian blue sample from the temple of Seti I at Abydos, and they referred this to biodegradation process. The presence of paratacamite, atacamite, and brochantite may be resulted from the chemical alteration of cuprorivaite and because of the presence of Cl^- and S^{2-} ions (Kabbani, 1997; Smith & Clark, 2004).

4.2 Green pigment

The investigations of green samples by PLM prove the presence of pale or faded green particles and some of them are silica-rich. This may be a proof that the pigment is Egyptian green which is manufactured with the same components of Egyptian blue but with the varying their amounts and firing conditions. Unlike Egyptian blue, Egyptian green the amounts of lime are higher than the amount of copper; in addition to that the process is performed in a reducing condition with higher temperatures in the range of 950-1100°C. The produced color may be rich with silica or cupro-wollastonite $(Ca,Cu)_3$ (Si_3O_9) (Eastaugh et al., 2004; Hatton et al., 2008; Lau et al., 2008). The EDS and XRD analyses confirm this with the existence of cupro-wollastonite and plenty amounts of the rendering layer. Like the blue pigment samples, the presence of chloride and sulfate salts is attributed to the alteration of cupro-wollastonite into paratacamite, atacamite, and brochantite.

4.3 Red pigment

The photomicrographs obtained by PLM show some characterized features of red ochre; like the translucent/opaque red particles, which are associated with particles of quartz and other impurities. These particles are also characterized by variable particles size and shape (Eastaugh & Walsh, 2004). The former results agree with that provided by EDS analyses by the presence of Al, K, Fe, Mg and Si. By XRD analyses, hematite α-Fe_2O_3 is identified, in all analyzed samples, with different amounts of impurities especially clay minerals and quartz which the main feature of ochres in general (Calza et al., 2008). The samples contain the common salts which are kieserite, thenardite, and halite. Despite microcline is present in most of the rendering samples (Al-Emam et al., 2014); it may also be a constituent of red ochre (Calza et al., 2008; Calza et al., 2009; Jezequel et al., 2011). The mineral boehmite γ-AlO(OH) is detected in the three analyzed samples. Eastaugh et al. (2004) report that boehmite is often found in association with diaspore and gibbsite, lepidocrocite, hematite, goethite, kaolinite and halloysite. In addition, Mazzocchin et al. (2007) analyzed fragments of wall paintings from Istria, and boehmite was detected in both hematite and goethite.

4.4 Yellow pigment

The yellow pigments, under PLM, show the remarkable features of yellow ochre; as the particles differ in their size and shape, and associate with quartz and other particles. Both of EDS and XRD data prove the previous results; as all the samples contain goethite α-FeOOH, quartz and clay minerals. Yellow samples also contain other minerals, as: boehmite and hematite, in addition, they show the common salts. It should be clarified that the high amounts of calcite, gypsum and anhydrite may be attributed to the rendering layer.

4.3 Binder

All the data of FTIR analyses, of the archaeological samples, refer to the usage of gum Arabic as the organic binder in the mural paintings in both temples. This is due to the presence of the characteristic bands of polysaccharides and carbohydrates (Shearer, 1989; Derrick et al., 1999; Stuart, 2007). These data also agree with those of reference samples of gum Arabic and the analyzed ones by Attia (1995) from the temple of Seti I. Furthermore, gum Arabic was detected in many mural paintings belonging to the same dynasty; as Rickerby (1993) detected gum Arabic in the tomb of Nefertari, the preferable wife of Ramesses II, also it was also identified in the Royal Tomb of Amenophis III (Abd Elkawy et al., 2004). As well as, the detected binder in the tomb of Chapel of Menna (TT69) was gum (Garcia-Moreno et al., 2013). As a result, this may emphasizes the claim of Rickerby (1993) that gum binders were preferred by the ancient Egyptian artists in performing their mural paintings.

5. CONCLUSIONS

The variable techniques of examination and analysis provided a detailed identification of the paint layers of mural paintings of Seti I and Ramesses II temples at Abydos area. The results of these examinations and analyses could be pointed out as follows:

- the blue pigments consist of Egyptian blue,
- the green ones are of Egyptian green,
- the red pigments were mainly originated from red ochre,
- the yellow pigments were also from yellow ochre,
- and finally the binder is a polysaccharide compound which could be claimed to be gum Arabic.

All of these results agree, to a great extent, with those of other literatures which have been conducted on mural paintings belonging to the same period (18th Dynasty) in ancient Egypt.

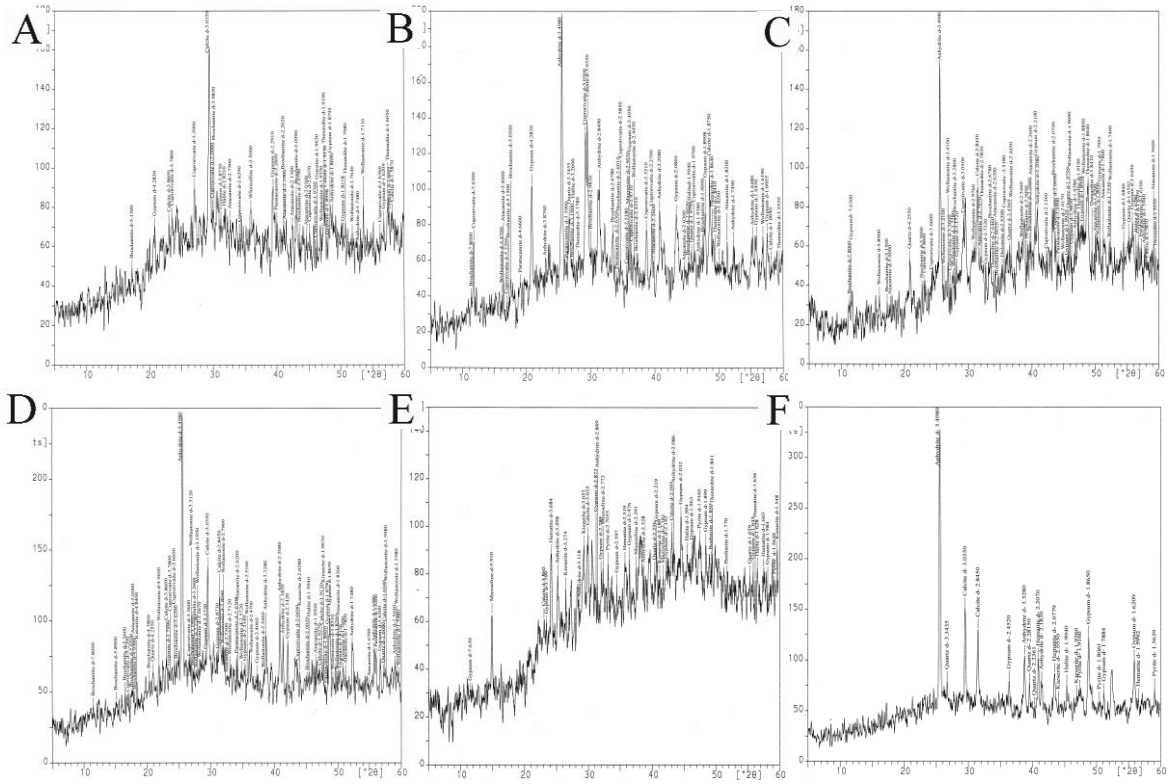

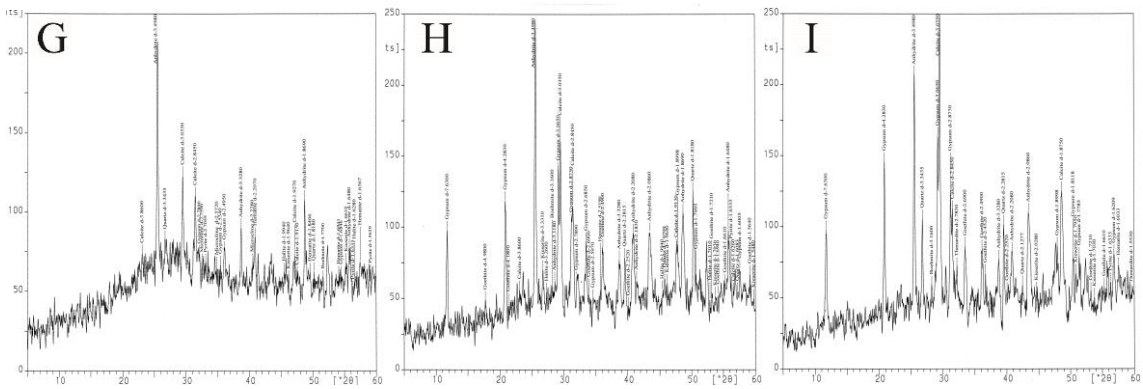

Figure 6: XRD pattern of different paint layer samples. *(A)* The blue sample (S6B). *(B)* The blue sample (ROB). *(C)* The green sample (S6G). *(D)* The green sample (ROG). *(E)* The red sample (S6R). *(F)* The red sample (RR1). *(G)* The red sample (RR). *(H)* The yellow sample (RKY). *(I)* The yellow sample (RY).

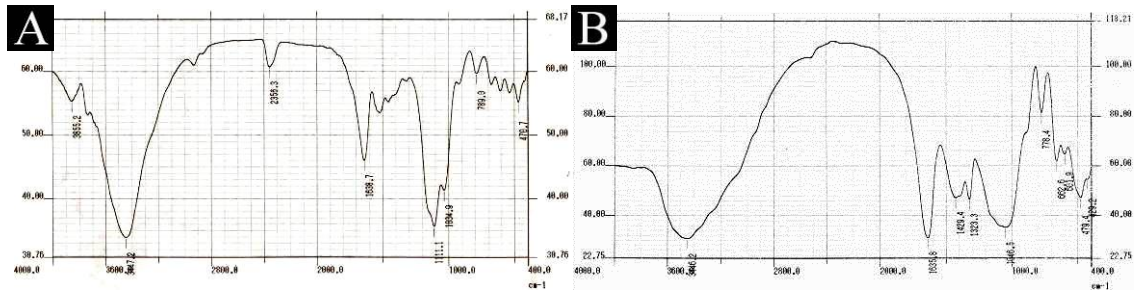

Figure 7: FTIR spectrum of: *(A)* the yellow sample (RY1) and *(B)* the blue sample (S6B).

REFERENCES

Abd El Aal, S. (2011). Identification of painting layers of Sennefer Tomb by Ion Beam Analysis. *Acta Physica Polonica, A., 120*(1), 144-148.

Abd Elkawy, A., Hassan, F., Kamil, P., Youhanna, W., Yoshimura, S., Nishisaka, A. (2004). Analyses of the pigments and plaster: Analyses of plaster and pigments' binding media conducted in the laboratory of the SCA. In S. Yoshimura, & J. Kondo, (Eds.), *Conservation of the Wall Paintings of The Royal Tomb of the Amenophis III: First and second phases report* (pp. 213-220). Tokyo: Waseda University.

Al-Emam, E., El-Gohary, M. & Abd El Hady, M. (2014). Investigations of mural paintings of Seti I and Ramesses II temples at Abydos – Egypt. *International Journal of Conservation Science, 5*(4), 421-434.

Al-Emam, E., El-Gohary, M., & Abd El Hady, M. (in press). *Photochemical degradation phenomenon: A case study on the mural paintings at Abydos Temples*.

Attia, H. R. (1995). *Study of treatment and conservation of Seti-I temple and memorial tomb "Osireion" in Abydos area*. (Master degree in Conservation & Restoration of Antiquities, Conservation Department, Faculty of Archaeology, Cairo University, Egypt), (in Arabic).

Bianchetti, P., Talarico, F., Vigliano, M. G., & Ali, M. F. (2000). Production and characterization of Egyptian blue and Egyptian green frit. *Journal of Cultural Heritage, 1*(2), 179-188.

Calza, C., Anjos, M. J., Mendonça de Souza, S. M. F., Brancaglion Jr, A., & Lopes, R. T. (2008). X-ray microfluorescence with synchrotron radiation applied in the analysis of pigments from ancient Egypt. *Applied Physics A, 90*(1), 75-79.

Calza, C., Pedreira, A., & Lopes, R. T. (2009). Analysis of paintings from the nineteenth century Brazilian painter Rodolfo Amoedo using EDXRF portable system. X-Ray Spectrometry, 38(4), 327-332.

Canti, M. G., & Heathcote, J. L. (2002). Microscopic Egyptian Blue (Synthetic Cuprorivaite) from Sediments at Two Archaeological Sites in West Central England. *Journal of Archaeological Science, 29*(8), 831-836.

Dasser, K. L. (1991). Pretreatment examination and documentation: The wall paintings of Schloß Seehof, Bamberg. In S. Cather, (Ed.), *The conservation of wall paintings: Proceedings of a symposium organized*

by the Courtauld Institute of Art and the Getty Conservation Institute, July 13-16, 1987 (pp. 103-135). London: The Getty Conservation Institute.

Derrick, M. R., Stulik, D., & Landry, J. M. (1999). *Infrared spectroscopy in conservation science*. Los Angeles: The Getty Conservation Institute.

Eastaugh, N., & Walsh, V. (2004). *The pigment compendium: Optical microscopy of historic pigments*. Amsterdam: Elsevier Butterworth-Heinemann.

Eastaugh, N., Walsh, V., Chaplin, T., & Siddall, R. (2004). *The pigment compendium: A dictionary of historical pigments*. Amsterdam: Elsevier Butterworth-Heinemann.

Hatton, G. D., Shortland, A. J., & Tite, M. S. (2008). The production technology of Egyptian blue and green frits from second millennium BC Egypt and Mesopotamia. *Journal of Archaeological Science, 35*(6), 1591-1604.

Garcia-Moreno, R., Hocquet, F.-P., Mathis, F., Van Elslande, E., Strivay, D., Vandenabeele, P. (2013). Archaeometry research on the wall paintings in the Tomb Chapel of Menna. In M. Hartwig, (Ed.), *The Tomb Chapel of Menna: The art, culture and science of painting in an Egyptian tomb* (pp. 93-113). Cairo: The American Research Center in Egypt.

Jezequel, P., Wille, G., Beny, C., Delorme, F., Jean-Prost, V., Cottier, R., . . . Despriee, J. (2011). Characterization and origin of black and red Magdalenian pigments from Grottes de la Garenne (Vallée moyenne de la Creuse-France): A mineralogical and geochemical approach of the study of prehistorical paintings. *Journal of Archaeological Science, 38*(6), 1165-1172.

Kabbani, R. (1997). Conservation a collaboration between art and science. *The Chemical Educator, 2*(1), 1-18.

Lau, D., Kappen, P., Strohschnieder, M., Brack, N., & Pigram, P. J. (2008). Characterization of green copper phase pigments in Egyptian artifacts with X-ray absorption spectroscopy and principal components analysis. *Spectrochimica Acta Part B: Atomic Spectroscopy, 63*(11), 1283-1289.

Lee, L., & Quirke, S. (2000). Painting materials. In P. T., Nicholson & I. Shaw (Eds.), *Ancient Egyptian materials and technology* (pp. 104-120). Cambridge: Cambridge University Press.

Lucas, A. and Harris, E. (1962). *Ancient Egyptian materials and techniques*. London: Arnold.

Marey Mahmoud H. (2012). A Multi-analytical approach for characterizing pigments from the Tomb of Djehutyemhab (Tt194), El-Qurna Necropolis, Upper Egypt. *Archeometriai Műhely*, 205-214.

Mazzocchin, G. A., Rudello, D., Bragato, C., & Agnoli, F. (2004). A short note on Egyptian blue. *Journal of Cultural Heritage, 5*(1), 129-133.

Mora, P., Mora, L., & Philippot P. (1984). *Conservation of wall paintings*. London: Butterworths.

Newman, R., & Serpico, M. (2000). Adhesives and binders. In P. T., Nicholson & I. Shaw, (Eds.), *Ancient Egyptian materials and technology* (pp. 475-494). Cambridge: Cambridge University Press.

Pavlidou, E., Marey Mahmoud, H., Roumeli, E., Zorba, F., Paraskevopoulos, K. M., & Ali, M. F. (2008). Identifying pigments in the temple of Seti I in Abydos (Egypt). In S. Richter & A. Schwedt, (Eds.), *EMC 2008 14th European Microscopy Congress 1–5 September 2008, Aachen, Germany* (pp. 829-830): Springer Berlin Heidelberg.

Rickerby, S. (1993). Original painting techniques and materials used in the Tomb of Nefertari. In M. A. Corzo & M. Afshar, (Eds.), *Art and eternity: the Nefertari wall paintings conservation project 1986-1992* (pp. 43-53). Los Angeles: The Getty Conservation Institute.

Robins, G. (2005). *The art of ancient Egypt* (Revised ed.). London: The British Museum Press.

Scott, D. A., Warmlander, S., Mazurek, J., & Quirke, S. (2009). Examination of some pigments, grounds and media from Egyptian cartonnage fragments in the Petrie Museum, University College London. *Journal of Archaeological Science, 36*(3), 923-932.

Shearer, G. L. (1989). *An evaluation of Fourier transform infrared spectroscopy for the characterization of organic compounds in art and archaeology*. (Doctoral thesis, University of London).

Smith, G. D., & Clark, R. J. H. (2004). Raman microscopy in archaeological science. *Journal of Archaeological Science, 31*(8), 1137-1160.

Stuart, B. H. (2007). *Analytical techniques in materials conservation*. England: John Wiley & Sons Ltd.

Uda, M., Sassa, S., Yoshimura, S., Kondo, J., Nakamura, M., Ban, Y., & Adachi, H. (2000). Yellow, red and blue pigments from ancient Egyptian palace painted walls. *Nuclear Instruments and Methods in Physics Research Section B: Beam Interactions with Materials and Atoms, 161–163*(0), 758-761.

Wiedemann, H.-G., Arpagaus, E., Müller, D., Marcolli, C., Weigel, S., & Reller, A. (2002). Pigments of the bust of Nefertete compared with those of the Karnak Talatats. *Thermochimica Acta, 382*(1–2), 239-247.